Local Effects of ECRH on Argon Transport in L-Mode Discharges at ASDEX Upgrade

M. Sertoli, C. Angioni, R. Dux, R. Neu, T. Pütterich and the ASDEX Upgrade Team

Max-Planck-Institut für Plasmaphysik, EURATOM Association, Garching, Germany

Introduction

Central impurity accumulation is a major concern for fusion devices since it leads to fuel dilution and excessive core radiative losses. The use of intense central electron wave heating has been proven a possible solution since it leads to an increase in impurity diffusivity and in some cases gives rise to outward impurity convection [1, 2, 3], but the underlying physics mechanisms are still not clear. Recent theoretical studies [4] predict the rise of a positive convection due to density fluctuations caused by parallel compression. The instability should be restricted to plasma regions with low safety factor q, low shear s and $R/L_{Te} > 2 \cdot R/L_{Ti}$. Since the last condition is not often encountered in the centre of H-mode plasmas, it is of major interest to investigate the operational space in which an outward convection may occur and to provide further experimental evidence to confute or confirm the existing theories.

A set of purely Electron Cyclotron Resonance heated (ECRH) Low-confinement mode (L-mode) experiments have been performed at ASDEX Upgrade (AUG) to study the dependence of the transport of argon (Ar) on the electron heating deposition profile. For a fixed total $\sim 1.2\ MW$ ECRH power delivered, different deposition radii have been tested, ranging from $\rho \sim 0.2$ to $\rho \sim 0.6$. Trace argon puffs have been performed during the flat-top of the discharges to evaluate the full profiles of the transport coefficients.

Determination of the argon transport coefficients

The Ar transport coefficients have been evaluated from the linear relation of the normalized Ar flux $\Gamma(r,t)/n(r,t)$ to the normalised Ar density gradient $1/n(r,t) \cdot \partial n(r,t)/\partial r$:

$$\frac{\Gamma(r,t)}{n(r,t)} = -\frac{D(r)}{n(r,t)} \frac{\partial n(r,t)}{\partial r} + v(r) \tag{1}$$

Diffusion (D) and convection (v) coefficients are flux-surface average quantities constant in time assumed equal for all ionization stages q of the impurity. This method is seldom applied because of the difficulty in evaluating experimentally the time evolution of the profile of the total impurity density. The novel solution to this problem proposed here (more in-depth in [5]) is the integrated use of the Soft X-ray (SXR) diode diagnostic, the Compact Soft X-Ray (CSXR) spectrometer and the 1D impurity transport code STRAHL. The method is explained for argon, but is applicable to any medium-high Z impurity.

The SXR diodes provide reliable medium-high Z emissivity profiles at high time and spatial resolution but without a trustworthy absolute intensity calibration. Since they integrate all the light in a certain spectral range ($\sim [1,20]\,keV$ for the present case), performing trace impurity puffs, the contribution of the puffed impurity to the detected emissivity can be recovered and modelled as $\varepsilon^{sxr}_{Ar}(r,t) = n_e(r)\, n_{Ar}(r,t)\, \sum_q f_{Ar,q}(r,t)\, k^{sxr}_{Ar,q}(r)$. The transport dependence of this equation is fully contained in the fractional abundance $f_{Ar,q}(r,t)$ and in the total impurity density profile $n_{Ar}(r,t)$, while the emissivity coefficients $k^{sxr}_{Ar,q}(r)$ are a function of n_e and T_e only. Sensitivity studies performed with STRAHL have demonstrated that $f_{Ar,q}(r,t)$ exhibits a low transport dependence which can be neglected in first approximation [5]. Simulating the Ar puff with STRAHL using a set of "typical" transport coefficients, the resulting $\varepsilon^{sxr}_{Ar}(r,t_{eq})$ at equilibrium can be divided by the total impurity density profile at the same time point obtaining a function $\varepsilon'(r)$ which contains all the information on the impurity emissivity characteristics (mapped on the equilibrium reconstruction of the discharge, accounting for the experimental n_e and T_e profiles) and is, within the assumptions made, completely decoupled from transport. The experimental $n_{Ar}(r,t)$ can be then evaluated by dividing the Abel-inverted, background-subtracted experimental SXR emissivity profile $\varepsilon^{exp}(r,t)$ at each time point by $\varepsilon'(r)$:

$$n^{sxr}_{Ar}(r,t) = \frac{\varepsilon^{exp}(r,t)}{\varepsilon'(r)} = \frac{\varepsilon^{exp}(r,t)}{n_e(r)\, \sum_q f_{Ar,q}(r,t)\, k^{sxr}_{Ar,q}(r)} \tag{2}$$

For sawtoothing plasmas, the background reference sawtooth cycle is subtracted from each cycle in the raw SXR data, thus guaranteeing that the n^{sxr}_{Ar} contains only contributions from Ar. The transport coefficients, extracted from inter-sawtooth cycles, are therefore intrinsically independent of the modelling of the sawtooth crash.

For the specific case of argon, $n^{sxr}_{Ar}(r,t)$ can be re-scaled through measurements from CSXR spectrometer to obtain an absolute measurement $n_{Ar}(r,t)$. Optimized for He-like Ar resonance lines, the CSXR spectrometer delivers an absolute LOS-integrated measurement of the Ar concentration $c_{Ar}(t)$. Since a mean radial localization $\overline{\rho}$ of this measurement can be evaluated by modelling the He-like Ar emission characteristics [5], equation 2 can be corrected:

$$n_{Ar}(r,t) = n^{sxr}_{Ar}(r,t) \cdot \frac{c_{Ar}(t_{eq}) \cdot n_e(\overline{\rho})}{n^{sxr}_{Ar}(\overline{\rho}, t_{eq})} \tag{3}$$

Results for ECR-heated L-mode discharges

The three L-mode discharges presented here have all been executed at $I_p \sim 800\,kA$, $\overline{n}_e \sim 3 - 4 \cdot 10^{19}\,m^{-3}$, $B_t \sim 2.3 - 2.4\,T$, using only $\sim 1.2\,MW$ ECRH as external heating power. For discharge # 24709, the full ECRH power was deposited at $\rho \sim 0.22$, for # 24916 at ~ 0.6 while for # 24648, $0.8\,MW$ were deposited at ~ 0.35 and the remaining $0.4\,MW$ at ~ 0.8. The sawtooth period was approximately constant at $\tau_{ST} \sim 20 - 30\,ms$, the inversion radii located at

$\rho_{inv} \sim 0.4$, 0.3 and 0.4 respectively. The profiles of the plasma parameters for all discharges (top plots in figure 1) show a strong change in T_e profile shapes (lines, top right) depending on the heating deposition and a slight peaking of n_e for off-axis and mixed heating (red and orange) with respect to full central deposition (blue). Since no NBI injection was performed in these discharges, the ion temperature profiles (dots, top right) have been inferred from the three measurement points available from the CSXR spectrometer and the Neutral Particle Analyser (NPA). The full T_i profile is therefore not precisely known, but an indication on T_e/T_i (> 3 for the centrally heated case) and on the R/L_T can anyway be extracted. The strong oscillations of R/L_{Te} (bottom right) for the centrally heated case (blue) are due to intense MHD activity, not present in the other two cases. To be noted is the $R/L_{Te} > 7$ in the region $\rho \sim 0.4 - 0.6$ for heating deposition within the $q = 1$ surface (blue and orange), approximately > 1.5 larger than for off-axis heating.

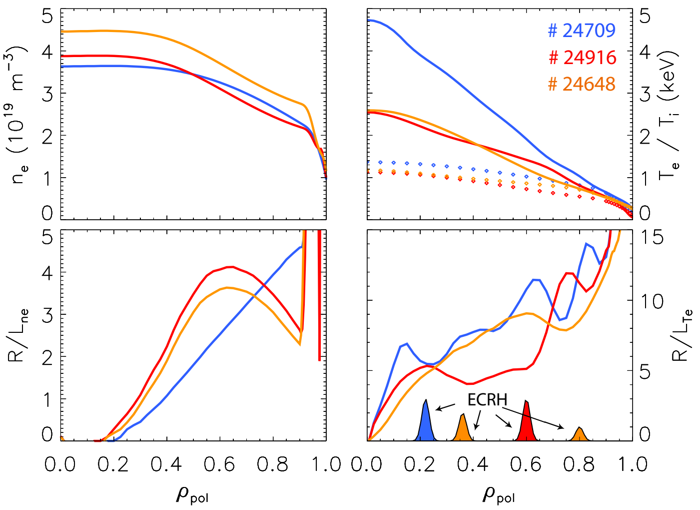

Figure 1: *Clockwise from top left: profiles of n_e, T_e (lines) and T_i (points), R/L_{Te}, R/L_{ne} for the three discharges labeled on the top right. Gaussians on the bottom right represent the ECRH deposition radii.*

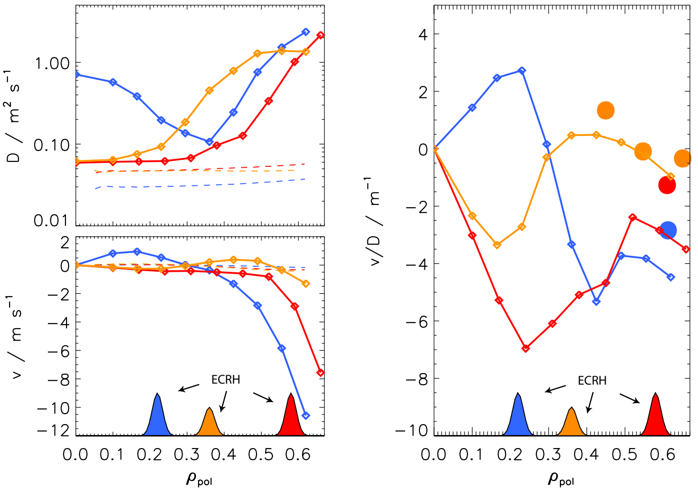

Figure 2: *Profiles of D (top left), v (bottom left) and v/D of Ar for the three discharges in figure 1. Dashed lines (right plots) are the neoclassical values evaluated through NEOART; large dots (right) the results from the GS2 simulations.*

The ECRH deposition position is found to have a strong influence on the profiles of the transport coefficients (figure 2). Taking the off-axis heating case (red) as reference, deposition within the sawtooth inversion radius (blue and orange) leads to a strong enhancement in the diffusion coefficient (top left) and to a transition of the convection velocity from negative to positive (bottom left) around the ECRH deposition radius, thus confirming previous experimental findings.

What is striking and novel of these results is the strong localization of these effects around the ECRH deposition radius. Sufficiently far from the ECRH deposition ($\rho < 0.2$ for the orange trace, $\rho > 0.4$ for the blue case), the diffusion coefficient approaches the reference values and is approximately neoclassical in the centre (red and orange). These results have been found in complete agreement with those from χ^2-minimization methods (modelling the sawtooth crash as a full flattening of n_{Ar} within the mixing radius) for the off-axis heating case and only in partial agreement for the other two cases. Since only the sawtooth crashes of the off-axis-heated discharge were "standard" [6], this is a further indication that the sawtooth modelling method is incomplete and often unsuited.

Simulations with the quasi-linear code GS2 have been performed with the plasma parameters in figure 1 only for radii greater than the sawtooth inversion radius so to be sure of the presence of nested flux-surface geometry necessary to excite the turbulent modes predicted by theory [4]. The decreasing trend of the drift parameter v/D (right in figure 2) for the orange case is qualitatively reproduced (full orange circles). For the on- and off-axis heating cases, the simulation underestimates the experimental absolute values by a factor ~ 2, although approximately reproducing the difference between the two discharges.

Conclusions

A novel methodology for the evaluation of the impurity transport coefficients through the linear flux-gradient relation of the total impurity density has been developed and applied to ECR-heated L-mode discharges at AUG. The method is intrinsically independent of sawtooth modelling and thus exhibits positive aspects in comparison to typical χ^2-minimization methods. Results indicate that central ECRH deposition leads to an enhancement of the diffusion coefficient and to the rise of a slightly positive convection. This confirms results from previous studies using independent methods and, additionally, shows that these effects are strongly localized around the ECRH deposition radius. These experimental results are found in promising qualitative agreement with quasi-linear gyrokinetic simulations with the code GS2.

References

[1] R. Dux et al., Plasma Phys. Controlled Fusion **45**(9), 1815–1825 (2003).

[2] R. Neu et al., Plasma Phys. Controlled Fusion **44**(6), 811–826 (2002).

[3] M. E. Puiatti et al., Phys. Plasmas **13**(4), 042501 (2006).

[4] C. Angioni and A. G. Peeters, Phys. Rev. Lett. **96**(9), 095003–1 (2006).

[5] M. Sertoli, PhD thesis, Ludwig-Maximilians-Universität München, 2010.

[6] I. Furno et al., Nucl. Fusion **41**(4), 403 (2001).